Processing fine powders by roll press

Vivien Esnault, Abderrahim Michrafy, Daniel Heitzmann, Mohamed Michrafy, Driss Oulahna

Processing fine powders by roll press

Vivien Esnault [a], Abderrahim Michrafy [b,*], Daniel Heitzmann [a], Mohamed Michrafy [c], Driss Oulahna [b]

[a] Lafarge Centre de Recherche, 95 rue de Montmurier, BP 15, 38291 St Quentin Fallavier, France
[b] Université de Toulouse, Mines Albi, CNRS, Centre RAPSODEE, Campus Jarlard, 81013 Albi, France
[c] BEM, Bordeaux Management School, 680 cours de la Libération, 33405 Talence, France

Keywords:
Roll compaction
Fine powders
Gas pressure
Modeling

A B S T R A C T

The gas trapped into fine powders causes specific problems like feeding disturbances during roll compaction process. In this study, the gas flow and its effect on the rolling process are numerically investigated in the rolling direction, using Darcy's law and assuming the permeability as a function of both material density and particle size through Carman–Kozeny relationship. The solid properties evolution is based on the Johanson model, whereas the solid speed is determined from the conservation of the material mass.

Computational results of solid properties and gas pressure distribution are presented by considering bentonite powder properties. According to material and process parameters, especially rolling speed and powder permeability, we discuss conditions for the escape of gas through the porous material during the process and stability conditions of the feeding at the rolls' entry.

Beyond the simplicity of the model (1D), it allows for a better understanding of fine powders processing by roll press. It highlights the combined effect of the permeability of the powder and the rotating speed on the gas pressure, during roll compaction process.

1. Introduction

Various technologies increasingly produce fine powders during processing and handling particulate matter. These fine powders cause specific problems like feeding and handling during their processing. Sometimes, the unwanted characteristic of fine powders needs to be changed in order to eliminate handling and dusting problems by increasing particle size, bulk density or modifying surface properties. In other situations, the main concern is to further reduce the particle size into extra-fine powders in order to increase the surface area and reactivity of powders. Both of the aforementioned goals can be achieved by processing the material by roll press.

Basically, the process operates as follows: the powder is fed to the compaction zone either by gravitational feeding or by a screw feeder. Then, the powder is drawn between two counter-rotating rolls in the stressing zone where the particle material undergoes fragmentation and/or consolidation.

Beyond the benefits of such compaction (continuous, economical and easy to use), the most common problems encountered are related to heterogeneity of strip properties due to the screw feeding system [1–4], and the gas trapped into the fine powders during stressing, generating pressure gradients which cause disturbances in the feed, noticeable changes of strip strength and process instabilities [5].

The effect of gas in the roller compaction is often emphasized in the literature. However, very little work has addressed the modeling of such effect. For e.g. the work of Johanson and Cox [4] presented an extension of the model for solid compaction [3] to predict gas transport and to include some considerations in process stability.

The problem of the gas trapped into fine powders and its escape by diffusing through the material is also encountered in other handling processes of powders such as the silo discharge, the screw feeding and the pneumatic conveying of powders. In contrast to roller compaction, studies on the effect of gas pressure in discharging or loading a silo of fine powders have been given more emphasis in the literature [1,2,6,7]. These studies were concerned in hopper design, or explored the effect of the geometry of the container and the length of time a given material takes to consolidate.

In the roll process, the situation seems to be more complex due to the evolution of the porosity of the material under roll pressure, and the inter-dependency between the process parameters and the powder properties.

In the present study, we investigate a model system describing the role of the gas flow in the feed powder during the rolling process through the analysis of gas pressure distributions. The model is based on the Johanson model for solid phase associated with the prediction of the solid properties [3], whereas the fluid transport through the porous material is assumed to obey Darcy's law, whereby permeability is a function of both material density and particle size through Carman–Kozeny relationship. The solid speed, which was not considered in the Johanson model but will be necessarily exploited in

* Corresponding author.
E-mail address: michrafy@mines-albi.fr (M. Michrafy).

Darcy's law, is derived from the basic conservation principle of mass. Considering the average values of cross-section of rolling, the formulation is essentially one-dimensional in space.

This work is organized into four sections. The model is derived in Section 2. The resulting system is non-linear, but weakly coupled (effect of gas pressure on the density evolution of the material is neglected in the compaction zone). In Section 3, the response of the solid under roll pressure is determined by solving the Johanson's equation. Having the average stress and density of the solid, the average gas pressure, which is described by an Ordinary Differential Equation (ODE), was solved using a finite differences scheme. Computational results, based on data of bentonite powder, are presented and discussed in Section 4. Finally, concluding remarks are presented.

2. The model

2.1. Solid behavior under roll compaction

For the prediction of the solid properties during rolling compaction, Johanson model was considered [3]. Extensive description and applications of this model can be found in [3,5,8–10]. In this approach, the powder behavior is assumed to be isotropic, frictional, cohesive and compressible and to obey the Jenike and Shield effective yield function [11]. The powder is characterized by internal friction angle δ and wall friction angle ϕ_w shown in Fig. 1. These properties are measured using a direct shear test, originally proposed in [12].

The average stress in the solid material is defined as:

$$\sigma_\theta = \frac{1}{2}(\sigma_1(\theta) + \sigma_2(\theta)) \tag{1}$$

where σ_1 and σ_2 are the major and minor principal stresses.

The mean normal stress σ_0 at the feed angle θ_0 is related to the pressure q_0 applied at the entrance of rolls (Fig. 2), as:

$$\sigma_0 = q_0(1-\sin\theta). \tag{2}$$

In the Johanson model, the feed angle θ_0 which depends on the material data and the wall friction parameters, is defined by:

$$\theta_0 = \frac{1}{2}(\phi_w + \arcsin(\sin\phi_w/\sin\delta)). \tag{3}$$

The feed powder is drawn between two counter-rotating rolls in the compaction zone where a high pressure is applied to deform the solid material. Drawing and densification of the powder in the compaction zone are based on the concept of the nip angle α, which defines two contiguous zones between rolls represented in Fig. 2. Before the nip angle named slip region, the powder is transported by relative sliding

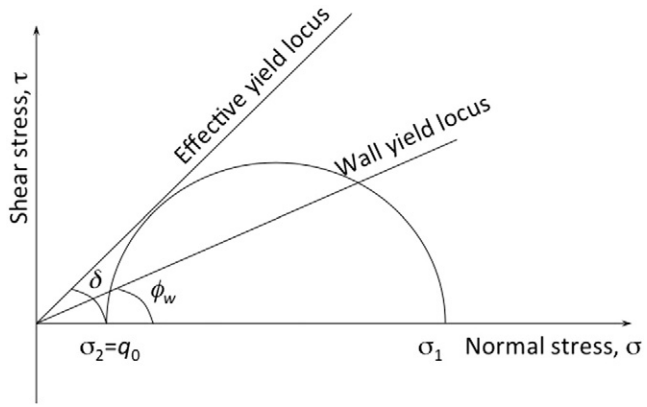

Fig. 1. Jenike and Shield effective yield function.

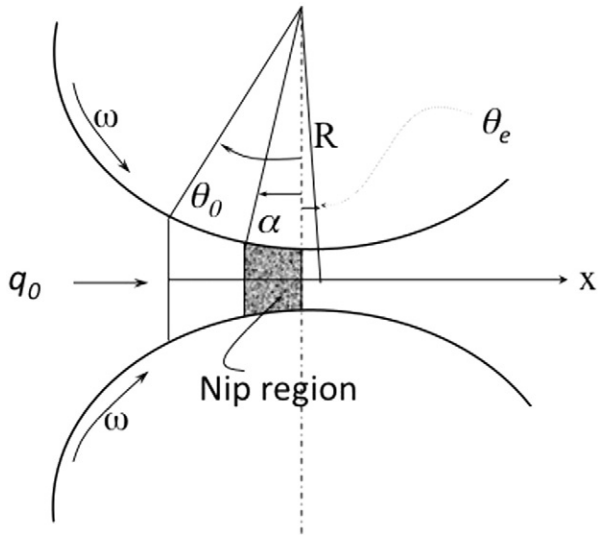

Fig. 2. Basic parameters of Johanson model (feed pressure q_0, nip angle α, feed angle θ_0, roll rotating angle, θ).

on the roll and obeys to the Jenike's yield criteria, and a slip condition at the rolls surface. Once the nip angle is achieved, the powder is assumed to be drawn by sticking to the roll surface and to be compacted by deforming under the high roll pressure near the gap. In this region, stress evolution can be calculated assuming adherence of the material on the walls. For linking density to the means stress, we adopt in this study following expressions:

$$\text{if } \sigma_\theta < \sigma_\alpha \text{ then } \rho_\theta = \rho_0 \tag{4a}$$

$$\text{if } \sigma_\theta \geq \sigma_\alpha \text{ then } \rho_\theta = \rho_\alpha(\sigma_\theta/\sigma_\alpha)^{\frac{1}{\beta}}. \tag{4b}$$

Here, ρ_0 is the density at the feeding angle (assumed to be equal to the tapped density). The constant β is a material property representing the compressibility of the powder and is determined by simple compression test using a tablet press. The stress σ_α and the density ρ_α correspond to values at the nip angle α bearing in mind that Eq. (4a) assumes a tapped density before the nip angle.

The solid material is considered incompressible. The reduction of the volume under pressure is only due to the reduction of the porosity ϕ defined as:

$$\phi = 1 - \frac{\rho_\theta}{\rho_s} \tag{5}$$

where ρ_s is the true density of the solid. In Eq. (5), the porosity is a function of the rotating angle θ.

The determination of the density distribution needs the computation of the pressure distribution between rolls. Following the Johanson model [3], two solutions are considered for the stress gradient in the material, assuming that slip either occurs or does not occur on the roll surface. The "slip" solution describes the situation in the "slip zone", when the "stick" solution describes the situation in the nip zone. The nip angle is determined using a continuity argument on the stress gradient, and the stress solution for both zones can then be deduced. Finally, the pressure distribution between rolls is computed combining the two solutions before and after the nip angle.

It is known that this solution does not depend on the roll speed. As the speed parameter is needed for the computation of the gas pressure using Darcy's law, the solid velocity was derived from the conservation principle of mass. As the solution is in steady state, the quantity of solid is conserved in any eulerian slab of material in other words the flux of

solid is constant through any given fixed cross-section to the rolling direction:

$$(S + 2R(1-\cos\theta))(1-\phi(\theta))v_s = A \tag{6}$$

where S is the gap, R is the roll radius and A is a constant.

The constant A can be determined in the nip zone from the roll rotation speed ω in rpm, as there is no slip between the roll and the material. For instance, at the gap ($\theta = 0$), we have:

$$v_s(0) = \omega R. \tag{7}$$

Applying Eq. (7) into Eq. (6), the solid velocity could be expressed as:

$$v_s(\theta) = \omega SR(1-\phi(0))/(S + 2R(1-\cos\theta)(1-\phi(\theta)). \tag{8a}$$

This expression can similarly be written in a shorter form as:

$$v_s = \omega f(\theta) \tag{8b}$$

where $f(\theta) = SR(1-\phi(0))/[(S + 2R(1-\cos\theta))(1-\phi(\theta))]$.

2.2. Gas pressure in the porous medium

In addition to the above equations describing the roll compaction of the solid, continuity and constitutive equations of gas are to be added. In this approach, two assumptions are considered. First, the effect of gas pressure on the solid solution is neglected as in the compaction zone, the stress supported by the solid is several orders of magnitude higher than gas pressure. Second, as the average stress and density of the solid are considered, the analysis of the gas pressure is essentially one-dimensional in space. In the following, we introduce the variable $x = R\cos\theta$, showed in Fig. 1. Then the gradient follows as $\partial/\partial x = \frac{1}{R\cos\theta}\partial/\partial\theta$. The gas pressure could then be expressed, indifferently and without ambiguity, as a function of x or θ.

The continuity equation of the gas can be built in the same manner as for the solid phase. The gas conservation in any eulerian slab, provides a relation on the gas velocity v_g:

$$(S + 2R(1-\cos\theta))\phi(\theta)\rho_g v_g = \text{const}. \tag{9}$$

where ρ_g is the density of the gas. In Eq. (9), v_g represents the superficial velocity of gas.

In addition to the continuity equation, two constitutive equations are considered.

First, the gas is assumed to be ideal and isotherm (i.e. density ρ_g is proportional to the gas pressure P). Eq. (9) becomes:

$$P(\theta)(S + 2R(1-\cos\theta))\phi(\theta)v_g = \text{const}. \tag{10}$$

Second, pressure gradient and gas velocity are related through Darcy's law which can be written as:

$$\phi(\theta)\left(v_g - v_s\right) = \frac{K(\phi)}{\mu_g}\frac{\partial P}{\partial x} \tag{11}$$

where K is the permeability of the powder depending on the porosity and hence the position θ. The constant μ_g is the gas viscosity.

Darcy's law (Eq. (11)) is valid as long as the gas flow is slow enough to be considered laminar. This validity can be established by verifying that the Reynold's number $R_e = \frac{\rho_g}{\mu_g} v_g D_p$ is lower than 2 or 4 [13]. For fine powders with $D_p = 20\mu m$ and $\mu_g = 1.85\ E-5$ Pa. s, $\rho_g = 1.184$ kg/m^3 at 25 °C, Darcy law is applicable if v_g is lower than 4 m/s. However, in this study, where roll diameter press is 100 mm, the gas speed which are of the same order of magnitude as the superficial speeds of the roll, will not reach such a value unless the rolls are turning in the speed range of 400–800 rpm, which are excessive speeds.

Eliminating the gas velocity between Eqs. (10) and (11), it follows:

$$P(\theta)\quad S + 2R(1-\cos\theta))(\phi f(\theta) + \frac{1}{\mu_g}\frac{K(\phi)}{\omega}\frac{\partial P}{\partial x}\Big) = B \tag{12}$$

where B is a constant.

Knowledge of the permeability $K(\phi)$ is necessary to compute the gas pressure P. Its values could be determined experimentally for any powder of various porosities, and fitted by an empirical law. It was the approach chosen by Johanson and Jenike [1]. For this study, we prefer to adopt the widespread Carman–Kozeny relationship:

$$K(\phi) = \frac{\phi^3 D_p^2}{180(1-\phi)^2} \tag{13a}$$

$$D_p = \frac{6V_p}{S_p} \tag{13b}$$

where D_p is an average characteristic size of particles, computed from the ratio between the average characteristic volume V_p and the average characteristic surface S_p.

The use of Eq. (13a) is widely documented [13], and certainly is a good choice for permeability prediction in the absence of further characterization of the powder. It also has the great advantage of introducing the dependence of the permeability on the particle size in a comprehensive way.

However, there are concerns on the role of permeability and roll rotation speed on the gas pressure described in Eq. (12). As the porosity, computed from the Johanson solution of stress, does not depend on the roll rotating speed ω, the permeability (Eq. (13a)) is independent of ω. Then, from Eq. (12), it can be seen that the solution P depends on $K(\phi)$ and ω only through the ratio $\frac{K(\phi)}{\omega}$. This means that the model predicts the same gas pressure, for a proportional variation of the permeability and the roll rotation speed.

Finally, the above equations for the gas flow during the roll compaction process are completed by two boundary conditions:

$$P(\theta_0) = P_{atm} \tag{14}$$

$$\frac{\partial P}{\partial x}(0) = 0. \tag{15}$$

The first boundary condition is set when assuming that the gas is at atmospheric pressure at the feeding angle (in roller press, a space is generally provided between the feed system and the rolls to allow air to escape). In the case of a closed feeding system this might not be the case. If the air has to permeate through the material between the entry angle and any point at the atmospheric pressure, this could generate a pressure gradient that elevates the pressure at entry beyond this value. In this case, the present model could be adapted to take into account a model of the permeation through the feeding system.

The second boundary condition assumes that the pressure gradient is null at the gap. This corresponds to the situation where the flow of the gas is forced to be opposite to the flow of solid.

This assumption is acceptable as long as the quantity of gas escaping through the neutral position toward the release zone is neglected. Otherwise, the condition should be modified based on the assumption of atmospheric pressure condition at the release angle.

3. Numerical determination of solid and gas solutions

In this step, the pressure distribution σ_θ in the solid phase is first determined. Knowing the pressure distribution and the material compressibility β, the density distribution of the solid is computed

from Eqs. (4a)–(4b) and the determination of the porosity follows from Eq. (5). The last variable needed for the determination of the gas pressure in the porous medium, is the velocity of the solid v_s, which is simply calculated from Eq. (8a).

Having all of the above parameters, the gas pressure can be determined, during the roll compaction process, by solving Eqs. (12)–(15). As Eq. (12) is non-linear (due to the nonlinear term $P\frac{\partial P}{\partial x}$), no analytical solution seems evident. Eqs. (12)–(15) was then numerically solved.

A finite differences scheme was applied for the discretization of Eq. (12), assuming the initial value for the unknown constant B. Compliance to the boundary condition (Eq. (15)) then gives a value of gas pressure at the gap ($P(0) = B/SR\phi(0)$). From this value $P(0)$, a numerical solution of gas pressure is then computed in the interval $[0, \theta_0]$. However, the calculated gas pressure $P(\theta_0)$ does not meet, a priori, the boundary condition (Eq. (14)). The value of B, and hence $P(0)$, is then optimized through an iterative procedure until the boundary condition (Eq. (14)) is also met.

This numerical procedure is stable and converges rapidly. Finally, the gas pressure and its gradient are obtained.

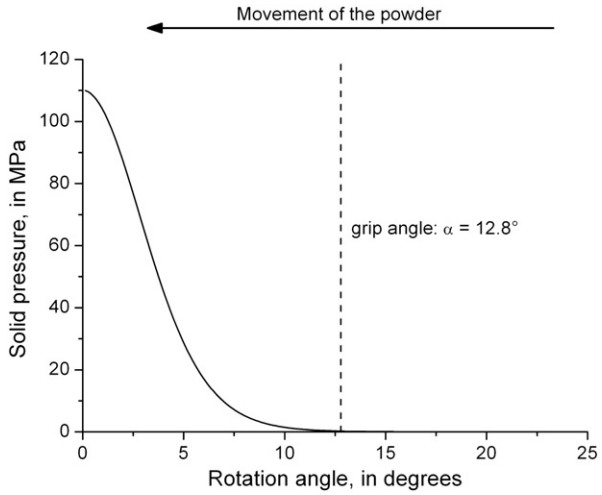

Fig. 3. Roll pressure distribution versus roll rotation speeds (bentonite powder).

4. Results and discussions

4.1. Material data and press parameters

The bentonite powder was used as a material example for this study. Its properties, characterized using common procedures as in [10], are summarized in Table 1. Particle size was calculated from the measured Blaine Specific Surface (BSS) through the relation $D_p = 6/\rho BSS$. Such D_p value is different than the measured mean particle size d_{50} using laser granulometry (Table 1).

Using Johanson model, simulations of roll compaction were carried out using a roll press diameter of 100 mm and a gap of 2 mm. The compaction is achieved with a maximum roll pressure of 110 MPa. The required feed pressure q_0 was determined accordingly, and the porosity at the feed angle θ_0 was determined from the tapped density as 0.65.

4.2. Pressure and porosity of the solid

The predicted roll pressure and porosity in the solid were plotted in Figs. 3 and 4. The feed angle of powder was set at 44°, however the plotted figures were limited to a rotating angle interval of 0–25. The nip angle was estimated to be 12.8°. The relatively high porosity (0.65) at the feed position, decreases under roll pressure up to 0.2.

4.3. Air pressure distribution versus roll rotation speed

From the above computed porosity and solid velocity during roll compaction, the gas pressure distribution was determined by solving the ODE. The viscosity of the gas (air) was taken as 1.85E − 5 Pa.s (in conditions of dry air at 25° and atmospheric pressure).

In Fig. 5, the gas pressure distribution is plotted at various roll rotation speeds. The higher values of the rotation speed are of course unrealistic, however the presented results show the diversity of situations that can arise in those systems.

In all cases, gas pressure builds up progressively starting from its entry between the rolls. By progressing toward the gap, the powder density increases and the space available for air is reduced. Some of the gas stays in the reduced space, contributing to the pressure rise, and some is evacuated through the incoming material (the appearance of fresh material).

Ultimately, the gas pressure profile depends on both the proportion of gas that is trapped in the porosity, and on the proportion that is evacuated.

A rotation speed of 0.95 rpm is considered to be either a low speed as such, or correlated to a very permeable powder. The escape of the gas through the powder is easily achieved either due to the high powder permeability which alternatively implies minimal resistance to gas movement, or due to the slow roll rotation speed which implies that the quantities of gas entrained are small. In both case (low roll speed or high powder permeability), named the “permeable limit case”, most of the gas escapes. Pressure build-up at the gap is minimal (Fig. 5). Pressure gradient at entry (the slope on curves in Fig. 6) is also very small, as the powder does not present an important resistance to the reduced quantity of air in movement.

A rotation speed of 66.7 rpm is considered to be either a high speed as such, or correlated to a very impermeable powder. Resistance to gas movement is high, or the gas quantities to evacuate are important due to the rotation speed. This situation where the most of air is trapped in the material is called the “impermeable limit case” in opposition to the “permeable limit case”. The pressure at the gap reaches very high values.

The compacted material can eventually undergo fragmentation prior to its release by the press [4,5]. In a not so intuitive manner, pressure gradient at the entry is also very small. As most of gas is trapped within

Table 1
Properties of bentonite powder.

Internal friction δ(°)	Wall friction ϕ_w(°)	Compressibility β	Blaine specific surface (cm2/g)	Average size of particles D_p (μm)
39	32	7.84	8000	2.84
True density (kg/m3)	Bulk density (kg/m3)	Tapped density (kg/m3)	Ribbon density (kg/m3)	Mean particle size d_{50} (μm)
2640	685	924	2112	7.4

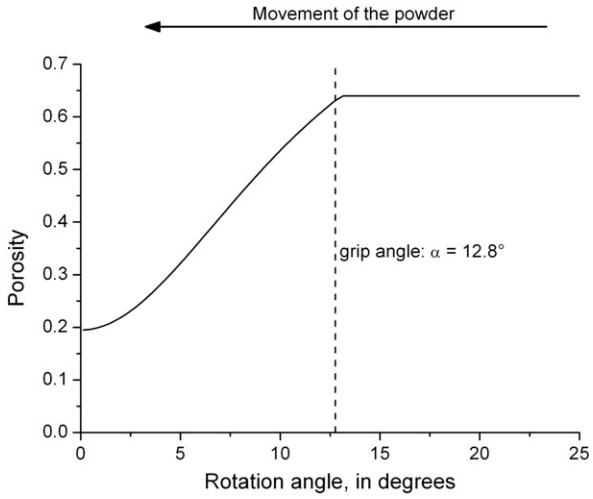

Fig. 4. Porosity distribution versus roll rotation speeds (bentonite powder).

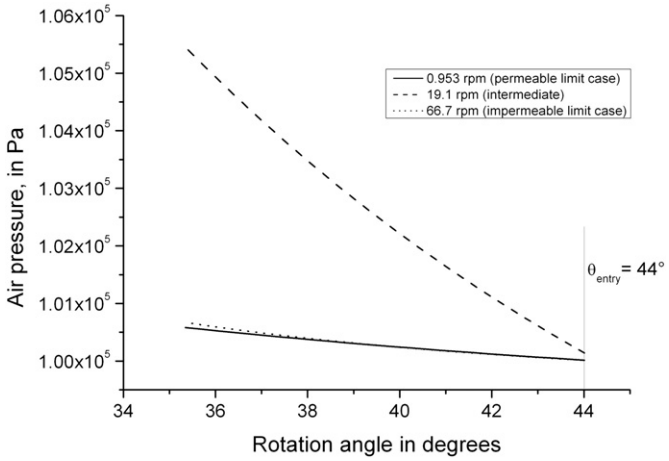

Fig. 6. Zoom on the gas pressure distribution at the roll feed.

the pores, the quantities of evacuated gas are not sufficient to create an important pressure gradient, at least near the entry.

4.4. Maximum gas pressure at the gap

Fig. 7 displays the maximum gas pressure for $\theta = 0$, as a function of the roll rotation speed. It confirms the previously stated result, i.e. gas pressure rise at the gap due to increased proportion of the air. The value reaches a limit, corresponding to the case where all the air initially present in the porosity is trapped in the compact.

In most applications, high gas pressure in the compacts is not acceptable as it can overcome the cohesion and damage the compacts when they are liberated from the stresses exerted by the press. Unfortunately, it is not possible to determine a general threshold value, as it depends on the compact cohesion (and then powder properties), and on process requirements.

4.5. Stability thresholds

The roll pressure in the gap forces the air to escape from the solid by compression. It results in the flow of most of trapped gas in the opposite direction to the solid flow, causing disturbances and instabilities of the feeding system. Otherwise, inside the press, particles are likely to be least affected due to the effort exerted by the rolls and the incoming feed. In order to analyze this effect, the dimensionless pressure gradient at the feed angle θ_0, defined as $DPG = \frac{\partial p}{\partial x}(\theta_0)/\rho_s g$, where ρ_s is the true particles density and g is the gravitational constant, is introduced as a measure of the effort exerted on the particles by the gas flow relative to their own weight.

In the case of gravity feeding, $DPG > 1$ will result in fluidization of the feed which causes process instabilities. In the case of screw feeding, $DPG > 1$ values can be reached due to the effort exerted by the feeding system, but Johanson and Cox [4], stated that $DPG > 10$ values are difficult to sustain even with screw feeding. In such a situation, a solution to partially eliminate air in the feed is required.

The dimensionless pressure gradient DPG calculated at the feed angle as a function of the rotation speed is plotted in Fig. 8. At the two extreme scenarios, i.e. very slow and very high rotation speeds, the DPG at the feed angle tends to 0 (stability zones). The highest values of DPG at the feed angle, which are the most likely to hinder the feeding system, are reached at intermediate gas pressure conditions when the resistance to air is high enough to lead to a high pressure gradient, but small enough to allow a sufficient quantity of air to be evacuated. This is the situation for rotation speed (19.1 rpm) in Fig. 5–6, where the maximum pressure is relatively high, but reached more progressively than in the impermeable case.

It is worth to mention that the predicted DPG values are very high due to the very high air content at feeding system. Small press

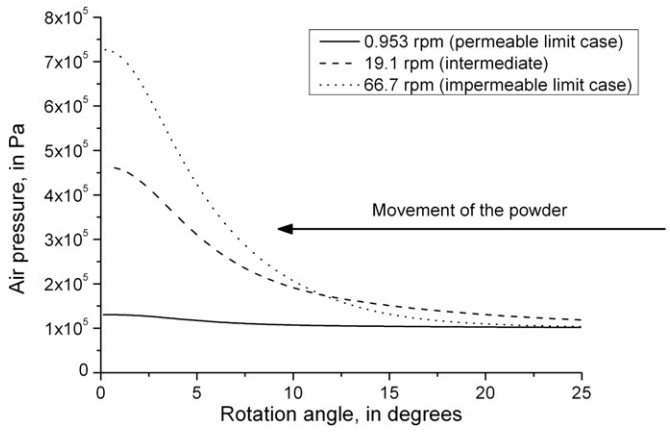

Fig. 5. Gas pressure distribution versus roll rotation speeds (case of the bentonite powder).

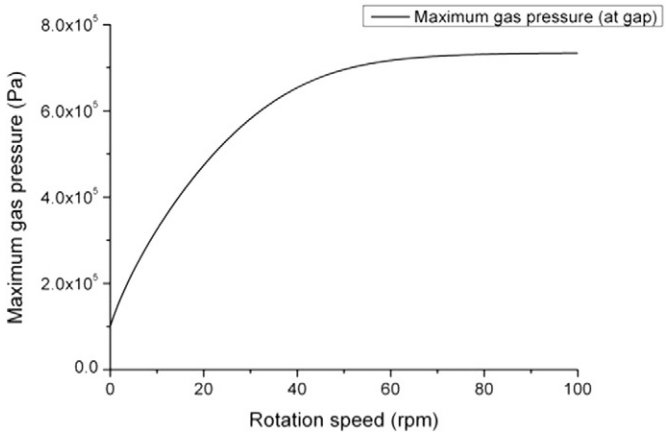

Fig. 7. Maximum gas pressure at the gap versus roll rotation speed (case of the bentonite powder).

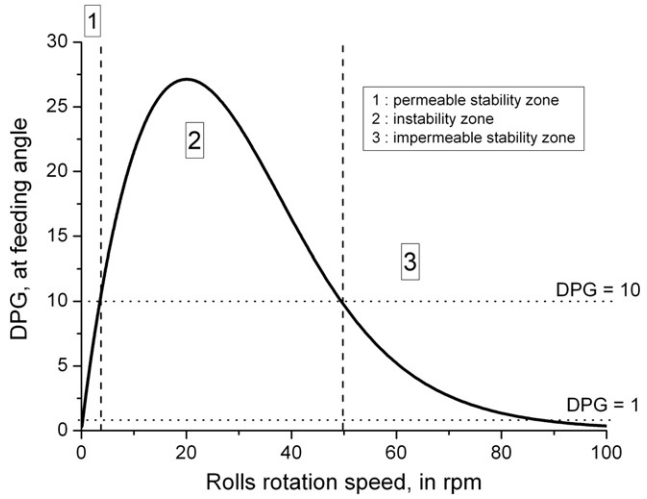

Fig. 8. Dimensionless pressure gradient $DPG = \frac{\partial P}{\partial x}(\theta_0)/\rho_s g$ at feed angle versus roll speed: stability zones (case of the bentonite powder).

dimensions ($D = 100$ mm) and boundary condition (Eq. (15)), which overestimates the gas pressure building effect, are another explanation.

5. Conclusion

A one dimensional model for gas flow during roll powder compaction was proposed, based on Johanson model for the computation of the solid stress and its porosity, and on Darcy's law for gas flow in the porous medium. The permeability was assumed as a function of porosity and particle size using Carman–Kozeny's law.

The predicted gas pressure for bentonite powder increases progressively from the feed angle toward the gap relating the increase of the powder density and hence, the reduction of the space available for gas. The importance of the ratio between permeability and roll rotation speeds, which determines the proportion of gas trapped within the compact, was discussed.

For the process stability, the model showed that, low dimensionless pressure gradient at the feed angle (DPG), can be obtained through both high and low values of permeability-roll rotation speed ratios. This result suggests that adapting the roll speed to the permeability of the powder could provide processing of fine powders by roll press.

The considered model does not allow predictions of all subtleties of the gas flow in the process. Also, the present study would greatly benefit from experimental confirmation.

List of symbols

$D = 2R$	roll diameter [mm]
S	gap [mm]
ω	rotational roll speed [rpm]
ρ_θ, ρ_s	apparent and true of solid [kg/m^3]
BSS	BLAINE Specific Surface [cm^2/g]
δ	internal friction angle [°]
ϕ_w	wall friction angle [°]
σ_θ	mean normal stress [Pa]
$\sigma_i(\theta), i = 1, 2$	major and minor principal stresses [Pa]
q_0	feed Pressure [Pa]
θ_0	feed angle [°]
ϕ	porosity [−]
v_s	solid velocity [m/s]
ρ_g	density of gas [kg/m^3]
v_g	superficial velocity of gas [m/s]
K	permeability [m^2]
μ_g	gas viscosity [Pa.s]
D_p	average size of particles [μm]
d_{50}	mean particle size [μm]
P	gas pressure [Pa]

References

[1] J.R. Johanson, A.W. Jenike, The effect of gaseous phase on pressures in a cylindrical silo, Powder Technol. 5 (1971) 133–145.
[2] P.G. Murfitt, P.L. Bransby, Deaeration of powders in hoppers, Powder Technol. 27 (1980) 149–162.
[3] J.R. Johanson, A rolling theory for granular solids, ASME J. Appl. Mech. 32 (1965) n°4.
[4] J.R. Johanson, B.D. Cox, Fluid entrainment effects in roll press compaction, Powder Handl. Process. 1 (1989) n°2.
[5] R.T. Dec, Problems with processing of fine powders in roll press, 24th Biennial Conference of the Institute for Briquetting and Agglomeration, vol. 241995. 199–210.
[6] K.A. Coffey, P.A. Gremaud, Numerical simulation of aerated powder consolidation, Int. J. Non-Linear Mech. 38 (2003) 1185–1194.
[7] J.R. Johanson, Modeling flow of bulk solids, Powder Technol. 5 (1971) 93–99.
[8] K. Sommer, G. Hauser, Flow and compression properties of feed solids for roll type presses and extrusion presses, Powder Technol. 130 (2003) 272–276.
[9] M. Balicki, Numerical methods for predicting roll press powder compaction parameters, Master's report, http://www.cs.jhu.edu/~marcin/conceptcatcher/projects/compaction/rpc_report.pdf 2003.
[10] G. Bindhumadhavan, J.P.K. Seville, M.J. Adams, R.W. Greenwood, S. Fitzpatrick, Roll compaction of pharmaceutical excipient: experimental validation of rolling theory for granular solids, Chem. Eng. Sci. 60 (2005) 3891–3897.
[11] A.W. Jenike, R.T. Shield, on the plastic flow of Coulomb solids beyond original failure, J. Appl. Mech. 26 (1959) 599–602.
[12] A.W. Jenike, P.J. Elsey, R.H. Woolley, Flow properties of bulk solids, ASTM proceeding, 601960. 1168–1181.
[13] F.A.L. Dullien, Porous media fluid transport and pore structure, Academic press, San Diego, 1992..